

AFRRI — TECHNICAL REPORT



Rat phantom depth dose studies in electron, X-ray, gamma-ray, and reactor radiation fields

**M. Dooley
D. M. Eagleson
G. H. Zeman**

DEFENSE NUCLEAR AGENCY

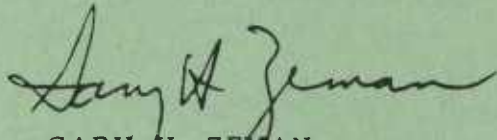
ARMED FORCES RADIOBIOLOGY RESEARCH INSTITUTE

BETHESDA, MARYLAND 20814-5145

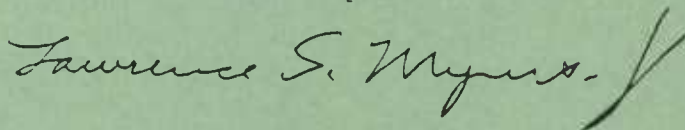
APPROVED FOR PUBLIC RELEASE; DISTRIBUTION UNLIMITED

TR86-5

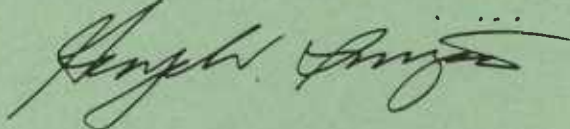
REVIEWED AND APPROVED



GARY H. ZEMAN
CDR, MSC, USN
Chairman
Radiation Sciences Department



LAWRENCE S. MYERS, Ph.D.
Scientific Director



GEORGE W. IRVING, III
Col, USAF, BSC
Director

REPORT DOCUMENTATION PAGE

1a. REPORT SECURITY CLASSIFICATION UNCLASSIFIED		1b. RESTRICTIVE MARKINGS		
2a. SECURITY CLASSIFICATION AUTHORITY		3. DISTRIBUTION/AVAILABILITY OF REPORT Approved for public release; distribution unlimited.		
2b. DECLASSIFICATION/DOWNGRADING SCHEDULE				
4. PERFORMING ORGANIZATION REPORT NUMBER(S) AFRRI TR86-5		5. MONITORING ORGANIZATION REPORT NUMBER(S)		
6a. NAME OF PERFORMING ORGANIZATION Armed Forces Radiobiology Research Institute	6b. OFFICE SYMBOL (If applicable) AFRRI	7a. NAME OF MONITORING ORGANIZATION		
6c. ADDRESS (City, State and ZIP Code) Defense Nuclear Agency Bethesda, Maryland 20814-5145		7b. ADDRESS (City, State and ZIP Code)		
8a. NAME OF FUNDING/SPONSORING ORGANIZATION Defense Nuclear Agency	8b. OFFICE SYMBOL (If applicable) DNA	9. PROCUREMENT INSTRUMENT IDENTIFICATION NUMBER		
8c. ADDRESS (City, State and ZIP Code) Washington, DC 20305		10. SOURCE OF FUNDING NOS.		
11. TITLE (Include Security Classification) (see cover)		PROGRAM ELEMENT NO. NWED QAXM	WORK UNIT NO. MJ 00137	
12. PERSONAL AUTHOR(S) Dooley, M., Eagleson, D. M., and Zeman, G. H.				
13a. TYPE OF REPORT Technical	13b. TIME COVERED FROM _____ TO _____	14. DATE OF REPORT (Yr., Mo., Day) December 1986	15. PAGE COUNT 19	
16. SUPPLEMENTARY NOTATION				
17. COSATI CODES		18. SUBJECT TERMS (Continue on reverse if necessary and identify by block number)		
FIELD	GROUP			SUB. GR.
19. ABSTRACT (Continue on reverse if necessary and identify by block number)				
High energy electrons, bremsstrahlung, and mixed neutron/gamma radiation fields are sometimes used in radiobiological experiments employing rats. This report describes the methods and results of a study of depth dose distribution in an acrylic rat phantom for each of these fields. Activation foils and thermoluminescent dosimeters were used to make the measurements.				
20. DISTRIBUTION/AVAILABILITY OF ABSTRACT UNCLASSIFIED/UNLIMITED <input type="checkbox"/> SAME AS RPT. <input type="checkbox"/> DTIC USERS <input type="checkbox"/>		21. ABSTRACT SECURITY CLASSIFICATION UNCLASSIFIED		
22a. NAME OF RESPONSIBLE INDIVIDUAL Junith A. Van Deusen		22b. TELEPHONE NUMBER (Include Area Code) (202)295-3536	22c. OFFICE SYMBOL ISDP	

CONTENTS

INTRODUCTION	3
METHODS	3
COBALT-60 FACILITY	3
LINAC	4
AFRRI TRIGA REACTOR	7
DEPTH DOSE MEASUREMENTS	10
RESULTS	12
DISCUSSION	15
CONCLUSIONS	15
REFERENCES	15

INTRODUCTION

Recent studies of the behavioral effects of ionizing radiation have revealed differing sensitivities of experimental animals that have been exposed to cobalt-60 photons, high-energy electrons, high-energy X rays, reactor neutrons, and reactor gamma rays (1,2). Electrons were found to be the most effective in reducing the performance capabilities of rats, and reactor neutrons the least effective. Although the reasons for these differences remain unknown, several factors relating to the physical characteristics of each source may be relevant. Among these factors are radiation quality, high-energy electron dose perturbations at anatomical interfaces, and temporal and spatial dose distributions within the animals.

The present study was performed to determine the characteristics of the spatial dose distributions in rat phantoms irradiated in each of the radiation fields mentioned above. The purpose of this investigation was to identify differences in the dose distribution patterns, which may have contributed to the results of the performance studies. Measurements were performed in acrylic rat phantoms in the Armed Forces Radiobiology Research Institute (AFRRI) cobalt-60 facility, linear accelerator (LINAC), and reactor using the same radiation fields as in the behavioral studies. Thermoluminescent dosimeters (TLD's) were used to measure the gamma-ray, electron, and X-ray dose profiles. Indium (In) and rhodium (Rh) activation foils were used to measure the neutron dose deposition. This report includes a description of the radiation fields, measurement techniques, and results, and a discussion of the measurements.

METHODS

COBALT-60 FACILITY

The AFRRI cobalt-60 facility (described in reference 3) consists of two sets of planar sources (total activity of ~64,800 curies as of November 1985) stored in a water-filled pool 1.8 meters wide by 4.9 meters deep. Irradiations can be performed either unilaterally by raising one source out of the pool, or bilaterally by raising the two sources simultaneously. The depth dose irradiations were performed unilaterally with the rat phantom placed inside a plastic rat holder and the midline of the phantom 28 cm from the outer edge of the source. Figure 1 shows the setup. For comparison, measurements were also made at a distance of 237 cm from the source (also unilateral irradiation).

Measurements to determine the midline tissue dose rate were performed in accordance with the protocol in reference 4, using a 0.5-cm³ tissue-equivalent (TE) ionization chamber placed midline in an acrylic rat phantom. Midline tissue dose rates of 20 Gy/min and 1 Gy/min were obtained at 28 cm and 237 cm, respectively, from the source.

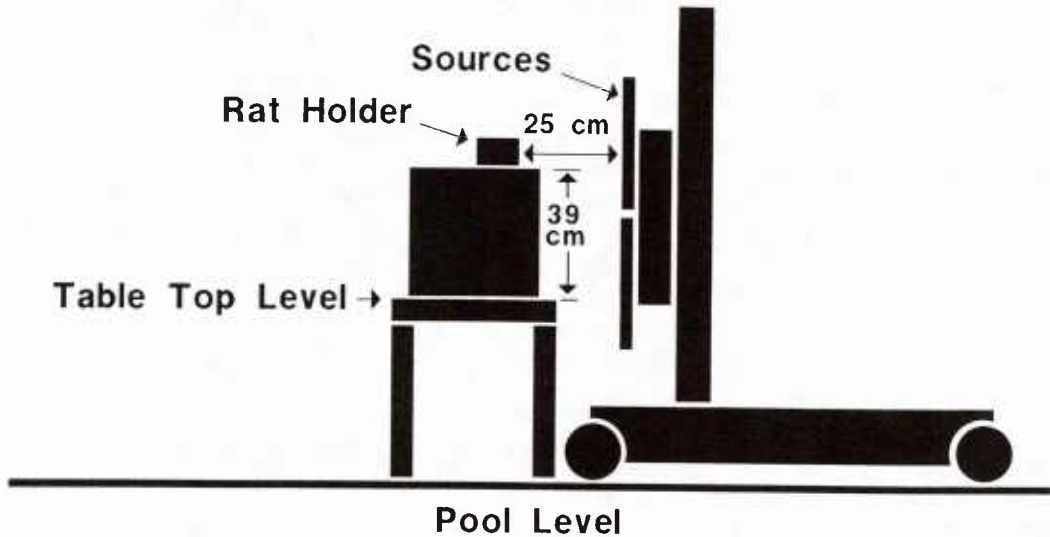


Figure 1. Rat phantom in cobalt-60 facility

LINAC

The AFRR I LINAC is described in reference 5. Depth dose characteristics were determined for the rat phantom irradiated with a beam of high-energy electrons, with initial energy of approximately 18.6 MeV and a beam of bremsstrahlung X rays with an average energy of about 6 MeV. The high-energy electron irradiations were performed with the phantom (inside a plastic rat holder) placed on a wooden table with the midline 4 meters from the LINAC beam port. A laser, previously aligned to the port center, was used to center the phantom in the electron beam (Figure 2). The bremsstrahlung spectrum was produced by accelerating 18-MeV electrons into a water-cooled converter consisting of seven tantalum foils, each 5 cm by 5 cm by 0.1 cm thick. A beam-flattening filter constructed of lead (diagrammed in Figure 3) was placed 84 cm from the beam port to improve beam uniformity. The phantom (in the plastic rat holder) was placed inside a 10-cm-thick paraffin cave to provide a uniform scatter environment, and a 2-cm-thick sheet of acrylic was placed in front of the array to ensure electronic equilibrium (buildup). Again, the laser was used to center the array 2.3 meters from the LINAC port. The array is shown in Figure 4.

The midline tissue dose rates for these configurations were measured using a 0.05-cm³ TE ionization chamber placed midline in a plastic rat phantom (5 cm diameter) and according to the procedures recommended in reference 4. Table 1 summarizes the radiation conditions.

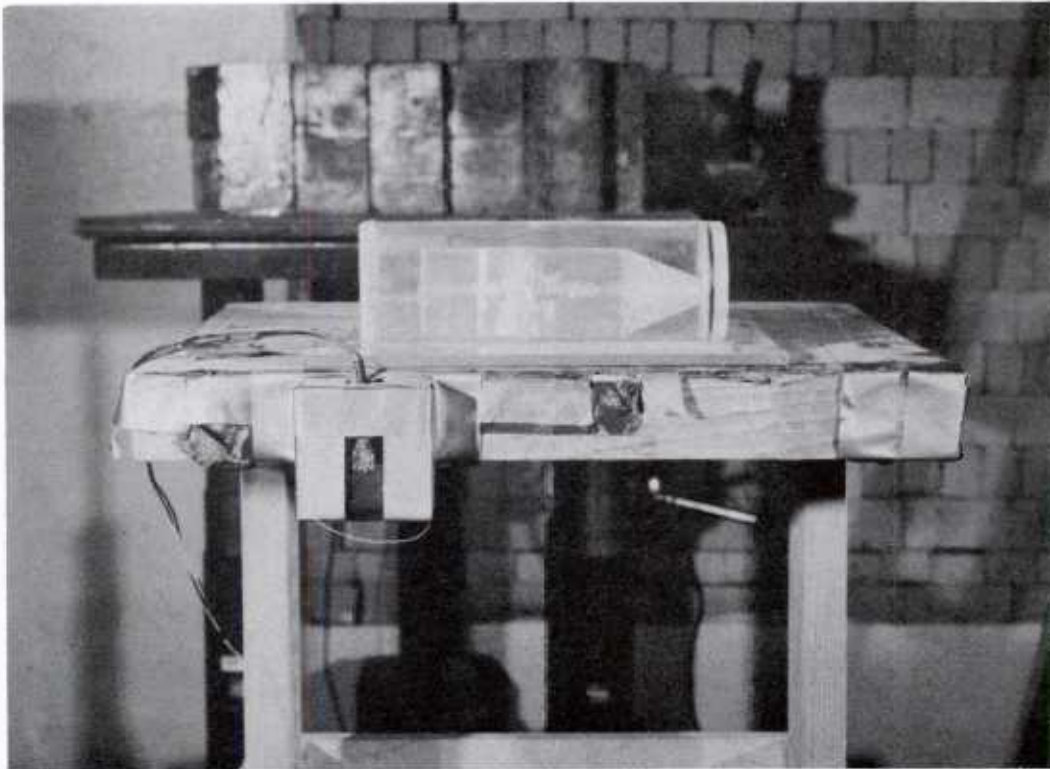


Figure 2. Rat phantom array for LINAC electrons

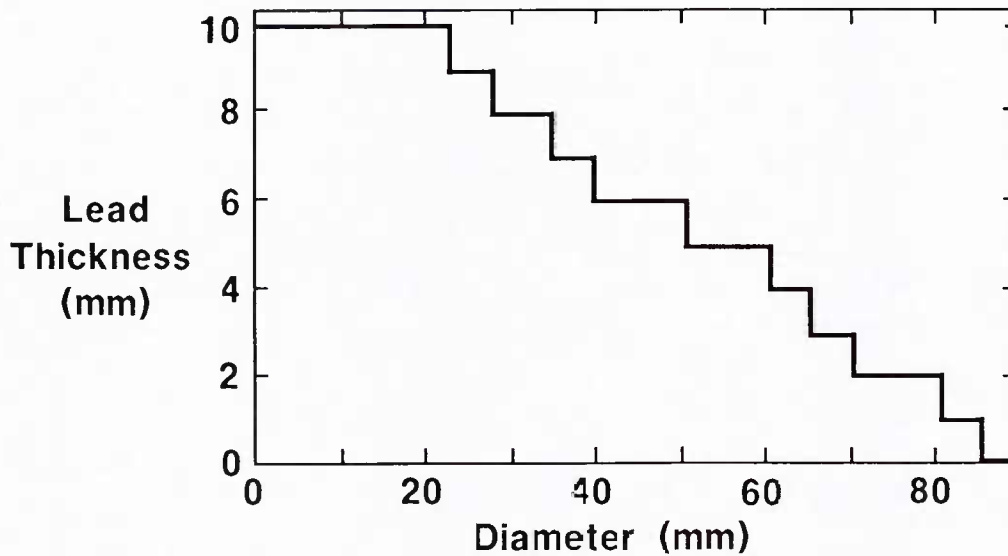


Figure 3. Flattening filter for LINAC 18-MVp X rays. Filter consisted of ten circular discs of 1-mm-thick lead stacked concentrically. Diameters of discs are shown in figure. In use, filter was centered in X-ray beam at 84 cm from LINAC port to project a uniform 25-cm-diameter field at 2.5 m from port.

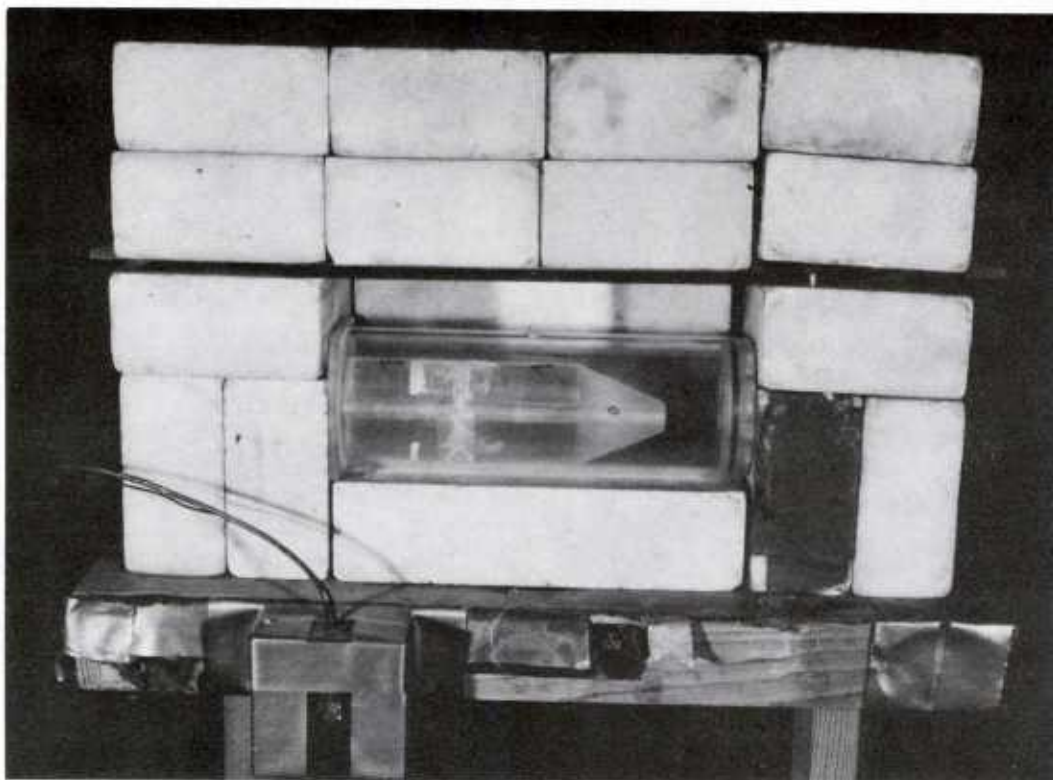


Figure 4. Rat phantom array for bremsstrahlung X rays

Table 1. LINAC Irradiation Parameters

	Midline Tissue Dose/Pulse (Gy)	Pulse Width (μ sec)	Instantaneous Dose Rate (Gy/Sec)	Pulse Per Sec	Average Dose Rate (Gy/Min)
Electrons	0.13	4	3.25×10^4	3	20
X rays	0.0055	4	1.37×10^3	60	20

AFRRI TRIGA REACTOR

The AFRRI reactor is described in references 6 and 7. It is a TRIGA (Training Research Isotopes General Atomic) Mark-F nuclear reactor, which is capable of operating in steady-state and pulsed modes. All measurements were performed in exposure room 1 (ER1) of the reactor facility using the rapid extractor system shown in Figure 5. The extractor system consists of an aluminum tube that extends from outside the exposure room through the west wall of ER1 to a position in front of the core. A polyethylene carriage attached to a pulley system is used to move specimens to and from the irradiation position. The rapid extractor system allows animals to be removed from the exposure room in just a few seconds rather than the 20 minutes (or more) otherwise required.

Five different reactor arrays were examined in this series of depth dose measurements. Each of the arrays has been used recently for radiobiology investigations. The arrays are as follows:

Standard high-neutron array. A 15-cm-lead (Pb) shield was used to attenuate most of the primary gamma rays. The extractor tube was centered 61 cm from the tank wall and 123 cm above the floor.

Modified high-neutron array. The extractor tube was centered 27 cm from the tank wall and 123 cm above the floor, and a Pb shield 15 cm thick and 30 cm high was constructed between the extractor tube and the tank wall.

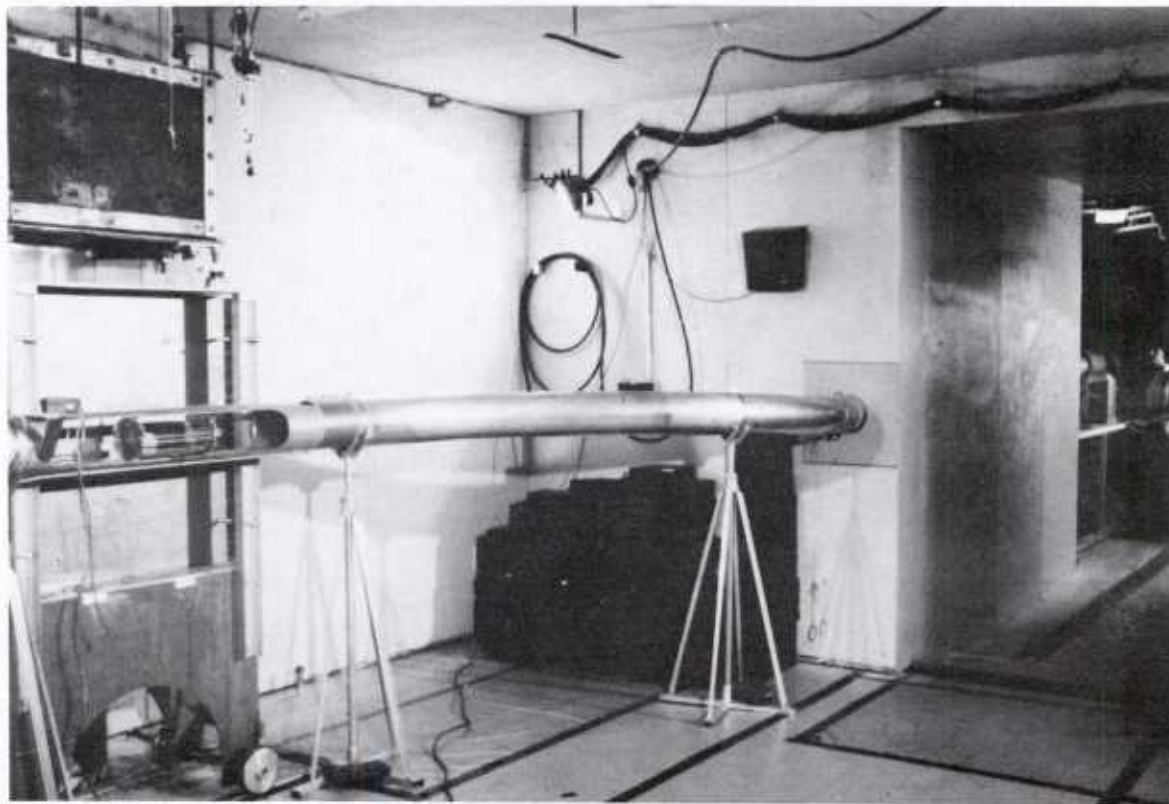


Figure 5. Rapid extractor system for AFRRI TRIGA reactor

Bare room. No shield was used (core in "full in" position), and the extractor tube was centered 61 cm from the tank wall and 123 cm above the floor.

Standard high-gamma array. The reactor core was backed up 30 cm in the pool, creating a water shield to attenuate most of the neutrons. The extractor tube was centered 61 cm from the tank wall and 123 cm above the floor.

Modified high-gamma array. The extractor tube was centered 27 cm from the tank wall and 123 cm above the floor, and the core was moved back behind 19 cm of water.

Different variations of the same basic fields were necessary in order to irradiate the rats to midline tissue doses ranging from 5 to 80 Gy in both the steady-state and pulsed modes. Providing a steady-state midline tissue dose rate of 20 Gy/min was relatively straightforward, since the reactor power could be varied until the desired dose rate was attained. However, the standard high-neutron and high-gamma arrays had to be modified to reach the high dose levels (~75 Gy) in the pulsed mode.

Table 2 summarizes the irradiation conditions for each array listed above. The midline tissue dose rates for the steady-state irradiations were measured according to the guidelines in reference 8, using paired 0.5-cm³ ionization chambers (TE chamber filled with TE gas and magnesium chamber with argon gas) placed inside a tissue-equivalent (A-150 plastic) rat phantom. For the pulsed radiations, a 0.05-cm³ TE chamber with TE gas was substituted because it did not demonstrate significant saturation in the pulsed fields. The 0.05-cm³ chamber measured total dose, and the neutron-to-gamma ratio measured in the steady-state mode was assumed to be the same for the pulsed mode. Note that the depth dose measurements were done only in the steady-state mode.

Table 2. Reactor Irradiation Parameters

Steady State	Midline Tissue Dose Rate (Gy/Min)			Power Level (kW)
	Neutron	Gamma	Total	
<u>15-cm-Pb shield</u>				
61 cm from tank wall	16.5	3.5	20.0	421
27 cm from tank wall	170.0	30.0	20.0	145
<u>Bare room</u>				
61 cm from tank wall	6.5	13.5	20.0	54
<u>Water shield</u>				
61 cm from tank wall*	—	20.0	20.0	400
27 cm from tank wall [§]	2.0	18.0	20.0	207
<hr/>				
<u>Pulsed</u>	Approximate Midline Tissue Dose/Pulse (Gy/MW · sec)		Range of Pulse Sizes (MW · sec) (~10 msec Pulse Width)	
<u>15-cm-Pb shield</u>				
61 cm from tank wall	0.86		—	
27 cm from tank wall	2.5		10.7-30.0	
<u>Bare room</u>				
61 cm from tank wall	6.1		5.7-12.8	
<u>Water shield</u>				
61 cm from tank wall*	2.2		—	
27 cm from tank wall [§]	4.2		4.5-17.8	

*30-cm-water shield

§19-cm-water shield

DEPTH DOSE MEASUREMENTS

All depth dose measurements were performed in 5-cm-diameter acrylic rat phantoms similar to the one shown in Figure 6. The phantoms were equipped with removable acrylic rods into which small cavities had been machined. TLD's or activation foils were placed in the cavities to measure the dose along lateral, longitudinal, and vertical axes of the phantom (Figure 7). Table 3 summarizes the types and number of dosimeters used in each field.

The dose distribution patterns in the cobalt-60 facility and LINAC facility were measured using Harshaw (Solon, OH) lithium fluoride (LiF) TLD-100 chips 3 mm by 3 mm by 1 mm thick. Reactor gamma-ray depth dose measurements were made with calcium fluoride (CaF) TLD-200 chips (same dimensions as the LiF chips) to take advantage of their low sensitivity to reactor neutrons. The phantoms, loaded with TLD's, were irradiated to a midline dose of approximately 5 Gy and read on a Harshaw Model 2000 D automatic TLD reader. Individual TLD responses at each position in the phantom were normalized to the response of the TLD chip midline in the phantom (position 12 in Figure 7). To enable better precision, the TLD's were sorted according to sensitivity to cobalt-60 photons before irradiation in the field of interest.

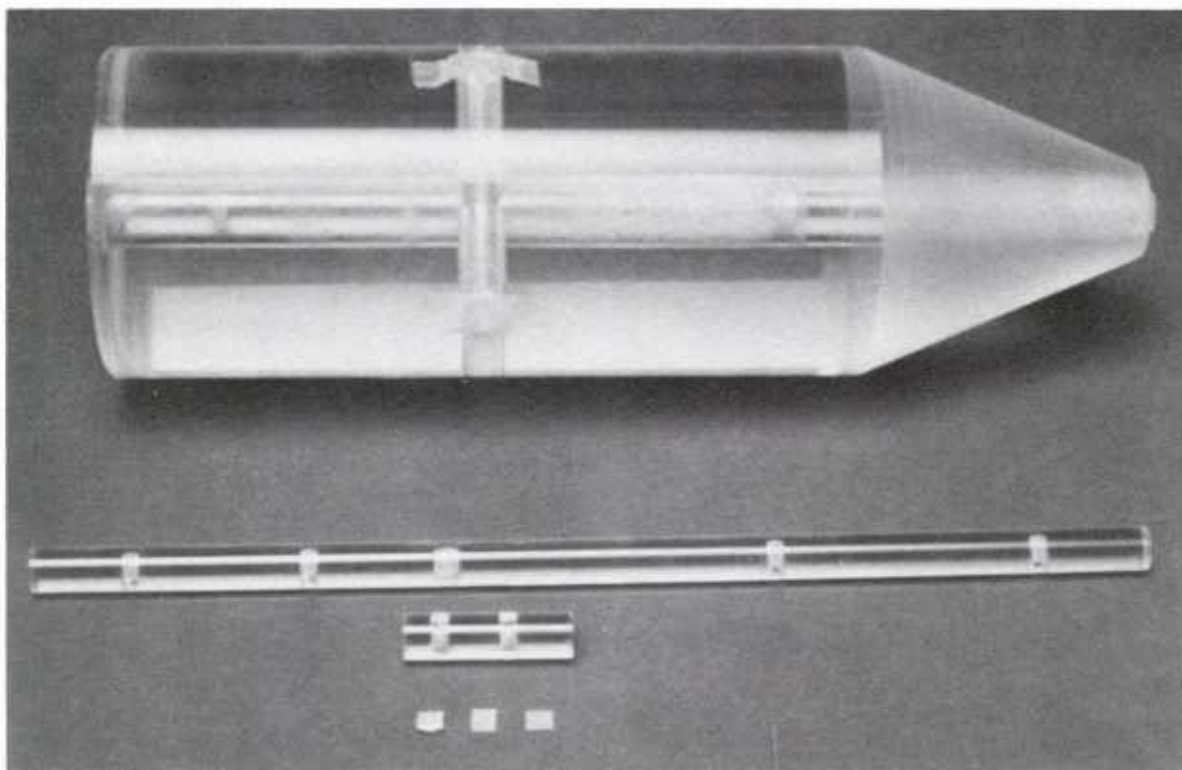


Figure 6. Acrylic rat phantom used for dosimetry measurements

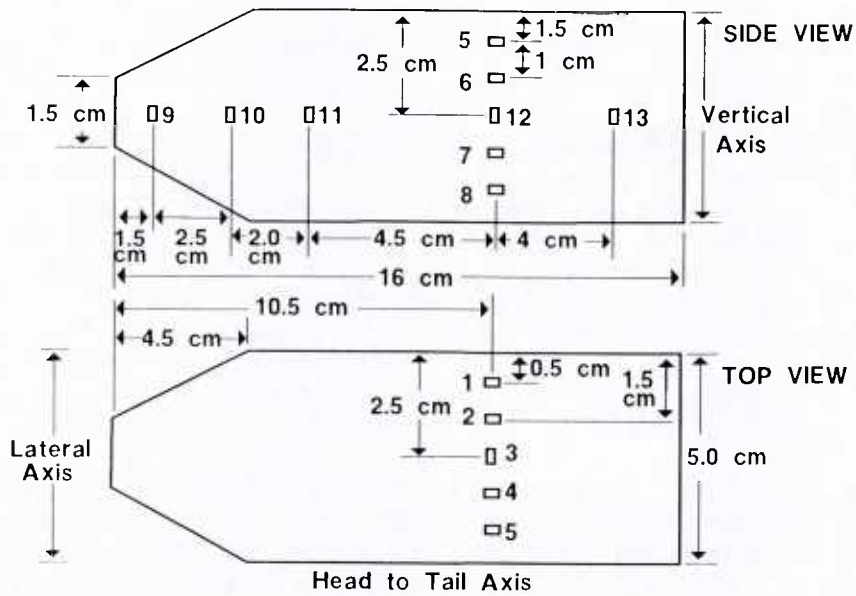


Figure 7. Diagram of axes of measurement in acrylic rat phantom

Table 3. Dosimeters Used in Measurements

Configuration	Dosimeters	Number of runs
<u>Cobalt-60</u>		
20 Gy/min	LiF TLD's	4
1 Gy/min	LiF TLD's	8
<u>LINAC</u>		
Electrons	LiF TLD's	8
X rays	LiF TLD's	8
<u>Reactor</u>		
15-cm-Pb shield:		
61 cm from tank wall	In foils	1
	Rh foils	1
	CaF TLD's	1
27 cm from tank wall	In foils	1
Bare:		
61 cm from tank wall	Rh foils	1
	CaF TLD's	2
Water shield:		
61 cm from tank wall*	CaF TLD's	4
27 cm from tank wall [§]	CaF TLD's	4

*30-cm-water shield

[§]19-cm-water shield

The neutron depth dose measurements were made with In and Rh activation foils placed inside the acrylic phantom. In and Rh were considered appropriate for these measurements because the shape of the reaction cross-section curves ($^{115}\text{In}[n,n']^{115m}\text{In}$ and $^{103}\text{Rh}[n,n']^{103m}\text{Rh}$) compares very well with that of neutron kerma in tissue for neutron energies between about 0.7 and 5 MeV (9). The foils were cut into squares of approximately 3 mm by 3 mm, and the In and Rh foils were 1 mm and 0.025 mm thick, respectively. Rh foils were covered with cadmium to shield the thermal neutrons and then irradiated to about 10 Gy (midline to the phantom). Instead of covering the In foils with cadmium, they were not counted until at least 10 half-lives of the ^{116m}In decay had elapsed. (^{116m}In results from the thermal neutron reaction with ^{115}In , $^{115}\text{In}[n,\gamma]^{116m}\text{In}$, which has a 54-minute half-life. The phantoms loaded with In foils were irradiated to a midline tissue dose of approximately 50 Gy.)

The 336-KeV gamma ray from the decay of ^{115m}In was counted using a high-purity germanium spectroscopy system, and a sodium iodide spectroscopy system was used to count the 20-KeV X rays from the decay of ^{103m}Rh . All results were normalized to the foil at the midline position of the phantom (position 12 in Figure 7).

RESULTS

The dose profiles in the different radiation fields are shown in Figures 8 through 11. Figure 8 shows the depth dose distributions through the rat phantom along the radiation beam axis. Figure 9 shows the dose variations across the length of the rat phantom. Figure 10 depicts the dose distributions on the vertical axis.

The precision for the cobalt-60 and LINAC irradiations was about 4%. However, due to positioning problems with the extractor carriage and the extremely small activation foils, the precision for the reactor gamma-ray and neutron measurements was only about 10%. With this precision, it was not possible to distinguish any significant differences in the depth dose curves of the different irradiation arrays. Consequently, the reactor neutron and gamma-ray data are plotted as the average of the reactor runs in the different configurations. Representative error bars are provided in Figure 8 to indicate the range of the reactor neutron and gamma data.

The depth dose profiles in Figure 8 indicate that the reactor neutrons are attenuated by a factor of about 2 through the rat phantom, while the other radiations are attenuated by only 5%-35%. LINAC electrons and bremsstrahlung X rays produce a very uniform distribution of dose across the diameter of the phantom, although the finite range of the electrons causes a rapid fall in dose, beginning near the exit surface of the phantom. The cobalt-60 curve is steeper than expected for 1.25-MeV gamma rays because these irradiations were performed at only 28 cm from the source, where the gamma-ray fluence is decreasing rapidly with distance. Figure 11 shows cobalt-60 depth dose data at 20 Gy/min (28 cm from the source) and at 1 Gy/min (237 cm from the source). This graph emphasizes that dose uniformity can sometimes be sacrificed for increased dose rates.

As indicated in Figures 9 and 10, the dose distributions from head to tail and from top to bottom are very uniform in all sources, with the exception of the electrons in Figure 10. Figure 10 shows a significant increase in dose to the "belly" of the animal, which is probably due to scatter from the wooden table that held the animals.

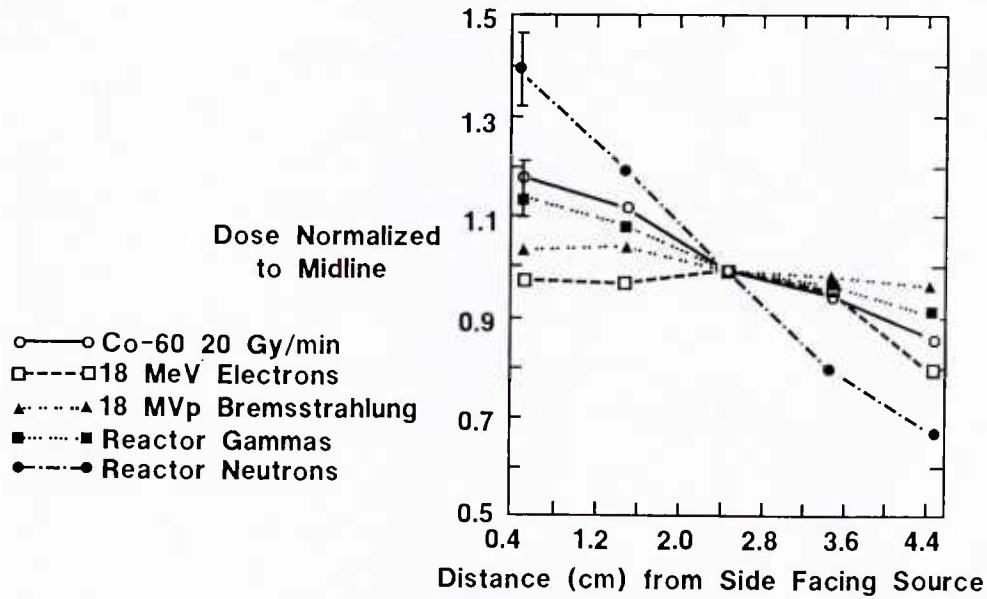


Figure 8. Depth dose on lateral axis (parallel to beam)

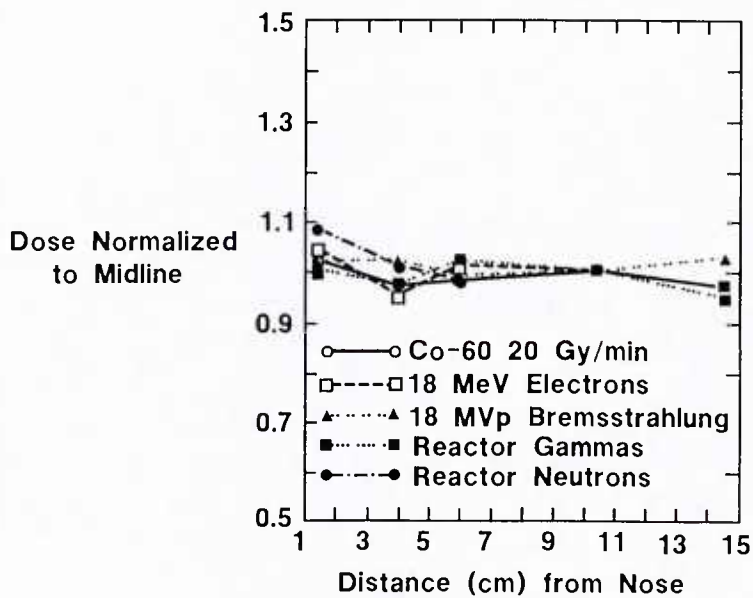


Figure 9. Depth dose on head-to-tail axis (across beam width)

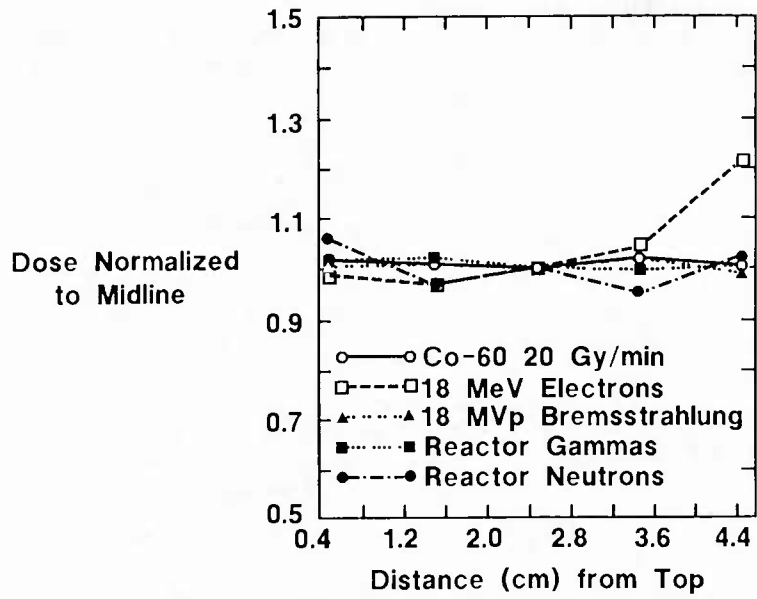


Figure 10. Depth dose on vertical axis (across beam height)

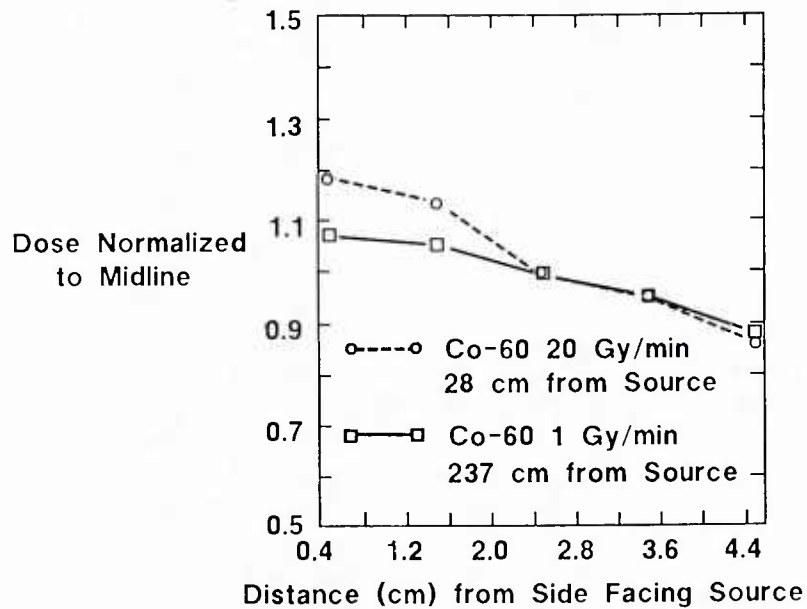


Figure 11. Cobalt-60 depth dose on lateral axis at 20 Gy/min and 1 Gy/min

DISCUSSION

The data presented in this report indicate that the depth dose profile of reactor neutrons in rats is significantly steeper than that of cobalt-60 gamma rays, LINAC electrons and bremsstrahlung X rays, and reactor gamma rays. These data agree well with other neutron depth dose studies (10, 11). However, more work is needed to determine if this is why the neutrons are less effective in producing performance decrement in irradiated rats. One means of eliminating the nonuniform neutron dose distribution would be to rotate the animals during neutron irradiation. A more uniform dose distribution would allow quantitative conclusions to be drawn on the relative effectiveness of neutron radiations and the lower LET radiations. Although questions remain concerning the significance of the depth dose distributions, it is important that the dose distribution patterns be evaluated for each irradiation condition, and that these patterns be considered when comparing results of studies performed in different sources.

A surprising result of these measurements was the increased dose to the "belly" of the electron-irradiated rats (Figure 10). Because the critical organ(s) in causing performance decrement has not been identified, the increase in dose to the gastrointestinal region of the rat may or may not be relevant. Simple changes in the experimental setup can be made, such as using a thin aluminum stand instead of the wooden table, to alleviate the nonuniform scattering. This would allow any future electron studies to be done without this potential artifact.

CONCLUSIONS

Dose distributions have been measured in rat phantoms in the following radiation fields: cobalt-60 gamma rays, high-energy electrons, high-energy X rays, reactor neutrons, and reactor gamma rays. The dose deposition patterns were measured on the midline of the lateral, longitudinal, and vertical axes of the phantom. Two major findings are as follows: (a) Significant differences exist in the neutron depth dose distribution compared to the other depth dose profiles. Reactor neutrons were attenuated by about a factor of 2 through the rat phantom, whereas the other radiations were attenuated by only 5%-35%. (b) It was discovered that the dose to the "belly" of the electron-irradiated rats was about 20% greater than the midline tissue dose. Except for these two findings, the dose distributions within the phantoms were relatively uniform, and they offered no clear explanation for the reported differences between behavioral sensitivities of rats exposed to different radiation fields.

REFERENCES

1. Bogo, V. Motor performance decrement in the rat produced by bremsstrahlung, electron, gamma, and neutron radiations. Presented at Thirty-Fourth Annual Meeting of Radiation Research Society, Las Vegas, Nevada, April 1986.

2. Hunt, W. A. Comparative effects of exposure to high energy electrons and gamma radiation on active avoidance behaviour. International Journal of Radiation Biology 44: 257-260, 1983.
3. Carter, R. E., and Verrelli, D. M. AFRRI cobalt whole-body irradiator. Technical Note TN73-3. Armed Forces Radiobiology Research Institute, Bethesda, Maryland, 1973.
4. Task Group 21 of AAPM. A protocol for the determination of absorbed dose from high energy photon and electron beams. Medical Physics 10(6): 741-771, 1983.
5. Gee, M. T. LINAC facility at Armed Forces Radiobiology Research Institute. Technical Report TR84-3. Armed Forces Radiobiology Research Institute, Bethesda, Maryland, 1984.
6. Sholtis, J. A., Jr., and Moore, M. L. Reactor facility at Armed Forces Radiobiology Research Institute. Technical Report TR81-2. Armed Forces Radiobiology Research Institute, Bethesda, Maryland, 1981.
7. Moore, M. L., and Elsasser, S. The TRIGA Reactor Facility at the Armed Forces Radiobiology Research Institute: A simplified technical description. Technical Report TR86-1. Armed Forces Radiobiology Research Institute, Bethesda, Maryland, 1986.
8. Goodman, L. J. A practical guide to ionization chamber dosimetry at the AFRRI reactor. Contract Report CR85-1. Armed Forces Radiobiology Research Institute, Bethesda, Maryland, 1985.
9. Zeman, G. H. Rhodium-103 and indium-115 inelastic scattering reactions for fission neutron dosimetry. Technical Report TR84-7. Armed Forces Radiobiology Research Institute, Bethesda, Maryland, 1984.
10. Verrelli, D. M. Dosimetry for neutron radiation studies in miniature pigs. Technical Note TN71-2. Armed Forces Radiobiology Research Institute, Bethesda, Maryland, 1971.
11. Serbat, A., and Dhermain, J. Experimentation de dosimetrie en mannequin du reacteur TRIGA de l'AFRRI (U.S.A.). ETCA-86-R-020, Etablissement Technique Central De l'Armement, Centre d'Etudes du Bouchet, 1986.